INSTITUTE OF PHYSICS PUBLISHING JOURNAL OF PHYSICS D: APPLIED PHYSICS
J. Phys. D: Appl. Phys. **39** (2006) 1793–1799 doi:10.1088/0022-3727/39/9/014

# Optical properties and structure of amorphous $(As_{0.33}S_{0.67})_{100-x}Te_x$ and $Ge_xSb_{40-x}S_{60}$ chalcogenide semiconducting alloy films deposited by vacuum thermal evaporation

**E Márquez[1,3], A M Bernal-Oliva[1], J M González-Leal[1], R Prieto-Alcón[1] and T Wagner[2]**

[1] Departamento de Física de la Materia Condensada, Facultad de Ciencias, Universidad de Cádiz, 11510, Puerto Real (Cádiz), Spain
[2] Department of General and Inorganic Chemistry, University of Pardubice, 53210, Pardubice, Czech Republic

E-mail: emilio.marquez@uca.es

Received 21 September 2005, in final form 17 January 2006
Published 20 April 2006
Online at stacks.iop.org/JPhysD/39/1793

**Abstract**
Amorphous films with compositions $(As_{0.33}S_{0.67})_{100-x}Te_x$ ($x = 0$, 1, 5 and 10 at.%) and $Ge_xSb_{40-x}S_{60}$ ($x = 10$, 20 and 30 at.%) have been prepared by thermal evaporation. The compositional dependences of their optical properties, with increasing Te and Ge content, respectively, are explained in terms of the modifications occurring in the film structure: Te joins the glassy network through the substitution of S atoms in the $AsS_3$ pyramidal units, to form new $AsS_2Te$ mixed pyramidal units, on the one hand, and, on the other hand, there is a presence of $GeS_4$ and $S_3Ge$–$GeS_3$ structural units, when the Ge content is increased. The refractive-index dispersion has been analysed on the basis of the Wemple–DiDomenico single-oscillator approach. It has been found that the refractive index increases in the As–S–Te system, with increasing Te content, while it decreases instead, in the Ge–Sb–S system, with increasing Ge content. The behaviour of the Tauc gap, when the composition of the material is varied, shows, as expected, just the opposite trends.

## 1. Introduction

The optical properties of chalcogenide vitreous semiconductors, such as excellent transmittance in the infrared region, continuous shift of the optical-absorption edge and values of the refractive index ranging between around 2.0 and 3.5, as well as a very strong correlation between the former properties and the corresponding chemical composition, explain the significant interest in these amorphous materials for the manufacture of filters, anti-reflection coatings and, in general, a wide variety of optical devices [1–3]. Furthermore, the broad range of photo-induced effects that the chalcogenide glasses exhibit [4,5], often accompanied by large changes in the optical constants [6,7], and, particularly, shifts in the absorption edge (i.e. photo-darkening or photo-bleaching), offer the possibility of using the chalcogenide glasses for high-density information storage and high-resolution display devices [8,9]. This clearly underlines the importance of the characterization of these glassy materials, by the accurate determination of their optical constants, refractive index, $n$, and extinction coefficient, $k$, as well as the corresponding optical band gap, $E_g^{opt}$.

The present paper is concerned with the systematic analysis of the optical properties and structure of as-deposited, amorphous $(As_{0.33}S_{0.67})_{100-x}Te_x$ (with $x = 0$, 1, 5 and

[3] Author to whom any correspondence should be addressed.

10 at.%), and $Ge_xSb_{40-x}S_{60}$ (with $x = 10$, 20 and 30 at.%) films, prepared by thermal evaporation. Despite the existence of a few reports in the literature concerning the structural properties of films within these two particular compositional lines, to the best of our knowledge, there is no thorough study of their optical properties and compositional dependences, as reported here.

## 2. Experimental details

Chalcogenide thin films were deposited using the vacuum thermal evaporation technique. To produce the bulk glass for the evaporation source, the constituents were measured into a quartz tube, vacuum sealed and melted in a rocking furnace for 24 h, at 920 °C, in the case of the $(As_{0.33}S_{0.67})_{100-x}Te_x$ samples and at 1000 °C, in the case of the $Ge_xSb_{40-x}S_{60}$ samples, and, subsequently, quenched in air. Fragments of the bulk material were then used to prepare the films in a vacuum chamber with a pressure of approximately $1 \times 10^{-4}$ Pa and at a rate of around 1 nm $s^{-1}$ (the deposition rate was continuously measured by the dynamical weighing procedure). X-ray diffraction showed that all the films to be studied were completely amorphous, and their chemical compositions were checked by EDX-analysis. The thicknesses of the films ranged between approximately 700 and 1200 nm, which are appropriate for the accurate evaluation of their optical parameters, by the *envelope* method that has been used in the present work, recently reported by González-Leal *et al* [10].

The optical-transmission spectra of the thin-film samples were measured, at normal incidence, over the 300 up to 2500 nm spectral region, by a double-beam, ratio-recording, UV/Vis/NIR computer-controlled spectrophotometer (Perkin Elmer, model Lambda-19). The spectrophotometer was set with a slit width of 2 nm. The area of illumination over which a single transmission spectrum was obtained is 1 mm × 10 mm. The absence of interference-fringe shrinking in those transmission spectra is clear evidence of the 'uniform-thickness nature' of the films [11], which were conveniently prepared using a 'planetary rotation' coating system (Tesla Co., model UP-858A). Such a thickness uniformity has also been confirmed by mechanical measurements, performed by a stylus-based surface profiler (Sloan, model Dektak 3030).

## 3. Results and discussion

### *3.1. Behaviour of the refractive index*

The transmission spectra of some representative amorphous As–S–Te and Ge–Sb–S thin-film samples under study are plotted in figure 1. Judging from these experimental results, a clear red-shift occurs in the interference-free region, with increasing Te content, while a blue-shift takes place, with increasing Ge content. Such shifts, as discussed later in this paper, are a consequence of the compositional dependences of the optical band gap. The values of the thickness, $d$, refractive index, $n$, and absorption coefficient, $\alpha$, of the films subjected to study have been determined *only* from their corresponding optical-transmission spectra, using

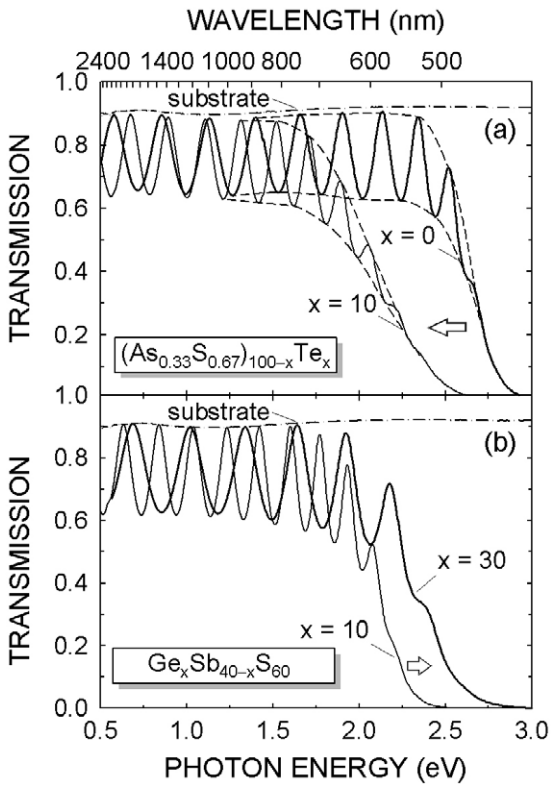


**Figure 1.** Optical-transmission spectra of some representative amorphous (*a*) $(As_{0.33}S_{0.67})_{100-x}Te_x$ and (*b*) $Ge_xSb_{40-x}S_{60}$ films, deposited onto *weakly-absorbing,* 1 mm-thick, borosilicate glass substrates (Menzel–Gläser microscope slides), by vacuum thermal evaporation. The transmission spectrum of the bare substrate is also plotted in both graphs. The top and bottom envelope curves have been computer drawn using the useful algorithm developed by McClain *et al* [12].

the previously mentioned, improved, envelope method, that interestingly, takes into account the weak absorption in the glass substrate (whose wavelength-dependent refractive index is around 1.51), in such a fashion that film-thickness values, with accuracies better than 2%, have been generally obtained—see table 1 in [10], where more detailed information about the accuracy of the film thicknesses can be found. Film-thickness results are all listed in table 1. Alternatively, these thicknesses were directly measured by the mechanical profilometer, and the differences between the mechanically-measured and the optically-calculated values were, in all the cases, less than 3%. In addition, it is necessary to clarify that the small loss in transmission between approximately 1400 and 600 nm, in the particular case of the $As_{33}S_{67}$ sample (see figure 1(*a*)), is a result of the equally small surface roughness, practically 'undetectable' with the optical-characterization method employed in this work.

On the other hand, this optical-characterization method provided values for the refractive index of the films, at the particular wavelengths where the transmission spectra are *tangential* to their corresponding top and bottom envelopes [11]. Moreover, the spectral dependence (dispersion) of the index of refraction was analysed in terms of the useful Wemple–DiDomenico (WDD) model [13, 14], which is based on the single-effective-oscillator approach and whose

**Table 1.** Values of the film thickness, $d$, WDD dispersion parameters, $E_0$ and $E_d$, static refractive index, $n(0)$, Tauc gap, $E_g^{opt}$, Tauc slope, $B^{1/2}$, and the band-tail width, $\Delta E_{tail}$, obtained for $(As_{0.33}S_{0.67})_{100-x}Te_x$ and $Ge_xSb_{40-x}S_{60}$ films under study.

| Composition | $d$ (nm) | $E_0$ (eV) | $E_d$ (eV) | $n(0)$ | $E_g^{opt}$ (eV) | $B^{1/2}$ ($cm^{-1/2}\,eV^{-1/2}$) | $\Delta E_{tail}$ (meV) |
|---|---|---|---|---|---|---|---|
| $As_{33}S_{67}$ | $961 \pm 7$ (0.7%) | $5.33 \pm 0.04$ | $21.46 \pm 0.18$ | $2.241 \pm 0.001$ | $2.50 \pm 0.01$ | $850 \pm 3$ | 81 |
| $As_{32.67}S_{66.33}Te_1$ | $866 \pm 7$ (0.8%) | $5.27 \pm 0.18$ | $21.41 \pm 0.72$ | $2.250 \pm 0.005$ | $2.45 \pm 0.01$ | $826 \pm 2$ | 86 |
| $As_{31.35}S_{63.65}Te_5$ | $1063 \pm 6$ (0.6%) | $5.02 \pm 0.03$ | $21.21 \pm 0.13$ | $2.287 \pm 0.001$ | $2.28 \pm 0.01$ | $690 \pm 3$ | 121 |
| $As_{29.70}S_{60.30}Te_{10}$ | $1182 \pm 15$ (1.3%) | $4.88 \pm 0.04$ | $20.80 \pm 0.19$ | $2.294 \pm 0.001$ | $2.08 \pm 0.01$ | $570 \pm 3$ | 176 |
| $Ge_{10}Sb_{30}S_{60}$ | $1177 \pm 5$ (0.4%) | $4.28 \pm 0.05$ | $21.79 \pm 0.23$ | $2.468 \pm 0.002$ | $1.97 \pm 0.01$ | $652 \pm 3$ | 121 |
| $Ge_{20}Sb_{20}S_{60}$ | $730 \pm 4$ (0.5%) | $4.51 \pm 0.08$ | $22.78 \pm 0.26$ | $2.459 \pm 0.002$ | $2.01 \pm 0.01$ | $605 \pm 2$ | 140 |
| $Ge_{30}Sb_{10}S_{60}$ | $952 \pm 6$ (0.6%) | $4.77 \pm 0.03$ | $23.88 \pm 0.17$ | $2.450 \pm 0.002$ | $2.10 \pm 0.01$ | $564 \pm 2$ | 161 |

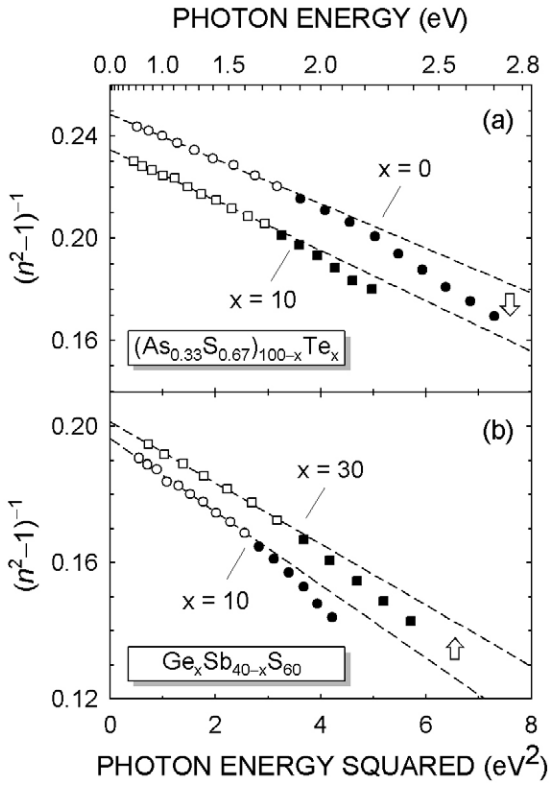


**Figure 2.** Plots of the refractive-index factor $(n^2 - 1)^{-1}$ versus $(\hbar\omega)^2$, of some representative amorphous (*a*) $(As_{0.33}S_{0.67})_{100-x}Te_x$ and (*b*) $Ge_xSb_{40-x}S_{60}$ films. Dashed straight lines are the corresponding linear least-squares fits. Solid circles represent those data departing from the linear behaviour, expected according to equation (1).

expression is

$$n^2(\hbar\omega) = 1 + \frac{E_0 E_d}{E_0^2 - (\hbar\omega)^2}, \qquad (1)$$

where $\hbar\omega$ is the photon energy, $E_0$ is the single-oscillator energy and $E_d$ is the so-called dispersion energy or single-oscillator strength. Plots of the refractive-index factor $(n^2 - 1)^{-1}$ *versus* $(\hbar\omega)^2$, for some representative ternary alloy films of the glassy systems under study, are shown in figure 2, along with their corresponding least-squares straight lines. It is worth emphasizing the goodness of the fits to the large-wavelength experimental data. The typical behaviour of the dispersion of $n$ is observed in all the cases: the experimental frequency variation in the refractive index clearly departs from that given by equation (1), when the photon energy approaches $E_g^{opt}$. Such a behaviour must be considered when choosing the set of data to be fitted to the WDD single-oscillator model, as an incorrect choice will certainly lead to erroneous values for $E_0$ and $E_d$.

Figure 2 shows that the departure from the linear trend occurs at lower photon energies, with increasing Te content, in the amorphous $(As_{0.33}S_{0.67})_{100-x}Te_x$ films, which indicates a decrease in the optical band gap, with increasing Te content. On the contrary, the departure from the linear trend takes place at higher photon energies, with increasing Ge content, in the case of amorphous $Ge_xSb_{40-x}S_{60}$ films, thus, evidencing an increase in $E_g^{opt}$, with increasing Ge content. Figure 2 also illustrates the influence of the chemical composition on the obtained values of the refractive index of the films, as the increase in Te content, leads to a decrease in the refractive-index factor, $(n^2 - 1)^{-1}$, stemming from the corresponding increase in the refractive index, while when the Ge content is increased, the trend is just the opposite.

The values of the WDD dispersion parameters, $E_0$ and $E_d$, for all the samples, were directly determined from the slope, $(E_0\ E_d)^{-1}$, and the intercept on the vertical axis, $E_0/E_d$, of their corresponding least-squares straight lines. Table 1 collects the values of these dispersion parameters, for all the samples subjected to study as well as the values of the static refractive index, $n(0)$, obtained by extrapolating equation (1) towards $\hbar\omega = 0$. In table 1 a decrease is observed in the dispersion parameter, $E_0$, for the amorphous As–S–Te films, with increasing Te content, while it rather increases in the case of the amorphous Ge–Sb–S samples, with increasing Ge content. The single-oscillator energy, $E_0$, is considered an *average* band gap, the so-called 'WDD gap', and it corresponds to the distance between the 'centres of gravity' of the valence and conduction bands: $E_0$ is, therefore, related to the average molar bond energy of the different bonds present in the material. Thus, the decrease observed in $E_0$ for the films belonging to the $(As_{0.33}S_{0.67})_{100-x}Te_x$ compositional line is due to the lower bond energy of the As–Te bonds (205 kJ $mol^{-1}$—all the bond-energy values mentioned in the present paper have been taken from [3]), in comparison with that corresponding to the As–S bonds (260 kJ $mol^{-1}$). Similarly, the increase observed in $E_0$ for the amorphous Ge–Sb–S films is a consequence of the higher bond energy of the Ge–S bonds (265 kJ $mol^{-1}$), when compared with that for the Sb–S bonds (230 kJ $mol^{-1}$).

The in-depth analysis of the dispersion of the refractive index, in terms of the WDD model, throws very valuable light on the structure of the material, through the values of the

oscillator strength, $E_d$. The set of values of $E_d$, belonging to the As–S–Te films (see table 1), shows a smooth decrease in $E_d$, with increasing Te content. Such a behaviour can be accounted for by considering the following empirical equation, proposed by Wemple and DiDomenico [13, 14]:

$$E_d = \beta N_c Z_a N_e \text{ (eV)}, \tag{2}$$

where $\beta$ is a two-valued constant, with either an 'ionic' or a 'covalent' value ($\beta_i = 0.26 \pm 0.03$ eV and $\beta_c = 0.37 \pm 0.04$ eV, respectively), $N_c$, the coordination of the cation nearest neighbour to the anion, $Z_a$, the formal chemical valency of the anion and, $N_e$, the total number of valence electrons (cores excluded), per anion. Thereby, when the Te content is increased in the amorphous $(As_{0.33}S_{0.67})_{100-x}Te_x$ films, $N_e$ decreases, as given by the following expression [14]:

$$\begin{aligned} N_e &= \{5 \times [0.33 \times (100 - x)] + 6 \times [0.67 \times (100 - x)] \\ &\quad + 6 \times x\}/\{[0.67 \times (100 - x)] + x\} \\ &= (567 + 0.33x)/(67 + 0.33x), \end{aligned} \tag{3}$$

where it has been considered that the number of valence electrons belonging to the As atom (cation) is certainly five and that corresponding to the S and Te atoms (anions) is six, while $\beta = \beta_c = 0.37 \pm 0.04$ eV and $Z_a = 2$ remain with the same values through the whole compositional line. Using equation (3) in order to obtain $N_e$, and the values for $\beta$ and $Z_a$, as well as the experimental values for $E_d$ listed in table 1, all of them in equation (2), values of 3.43, 3.43, 3.46 and 3.47, have been derived for the cation effective coordination number, $N_c$, for $x = 0$, 1, 5 and 10 at.%, respectively. So, an insignificant decrease is observed in $N_c$ when the Te content increases, which reflects that the concentration of the As–As homopolar bonds, present in the material, remains practically unchanged. It has been previously inferred from the Raman structural studies by Vlcek *et al* [15] that Te joins the structure of the amorphous $As_{33}S_{67}$ films, by substituting S atoms in the basic $AsS_3$ pyramidal structural units, forming the host matrix in this particular binary alloy, to form additional $AsS_2Te$ *mixed* pyramidal units. Since S and Te belong to the same group of the Periodic Table, group VIA, $N_c$ is not expected to change significantly by such an atom substitution, as experimentally found, since no breaking of pyramidal units occurs.

On the other hand, it has been determined that $E_d$ increases rather sharply, with increasing Ge content, in the case of the amorphous $Ge_xSb_{40-x}S_{60}$ films. Following a similar reasoning as the one done before, for the As–S–Te alloy films, a notable increase in $N_c$ is deduced for the Ge-based ternary alloy samples. In this case, the parameters on the right-hand side of equation (2) are $\beta = \beta_c = 0.37 \pm 0.04$ eV, $Z_a = 2$ and $N_e = [4 \times x + 5 \times (40 - x) + 6 \times 60]/60$, respectively. The values for $N_c$ belonging to the Ge–Sb–S glassy system are all listed in table 2.

It has to be noted that the $N_c$-values found experimentally, for the amorphous $Ge_xSb_{40-x}S_{60}$ films, are certainly consistent with those *theoretically* expected. In fact, if the chemical formula is rewritten as $(Ge_{0.025x}Sb_{1-0.025x})_{40}S_{60}$ and the 'hypothetical cation', $Ge_{0.025x}Sb_{1-0.025x}$, is considered in the analysis, the $N_c$-value is then given by the expression $N_c^{theo} = 4 \times (0.025x) - 3 \times (1 - 0.025x)$, as a function of Ge content. The values of $N_c^{theo}$ are also listed in table 2, and they are in fairly good agreement with those experimentally obtained. Nevertheless, it is observed that the experimental values are, in all the cases, slightly *smaller* than the theoretical ones, which is likely to be related to the presence of Ge–Ge and Sb–Sb homopolar bonds, as previously revealed by the Raman structural studies carried out by Kotsalas *et al* [16]. Amorphous stoichiometric $Sb_{40}S_{60}$ films have a similar structure to that of amorphous stoichiometric $As_{40}S_{60}$ films, which are both mainly formed by pyramidal units of the type $XS_3$ ($X$ = Sb or As). The addition of Ge to the $Sb_{40}S_{60}$ binary alloy produces a break in the stoichiometry, leading to both a 'cation build-up' and the subsequent formation of Ge–Ge and Sb–Sb homopolar bonds. It has also been shown by Kotsalas *et al* [16], that Ge–Ge bonds occur in $S_3Ge$–$GeS_3$ *modified* tetrahedral units, which have also been observed in amorphous $Ge_{40}S_{60}$ films. The concentration of these Ge–Ge homopolar bonds increases with increasing Ge content, providing further evidence for the slightly larger difference between the values of $N_c^{exp}$ and $N_c^{theo}$, for higher Ge contents. Finally, it should be pointed out that the increase found in the cation effective coordination number, for the Ge–Sb–S glassy system, is mainly due to the more and more significant presence of $GeS_4$ tetrahedral structural units (which coexist with the $SbS_3$ pyramidal structural units), with increasing Ge content.

**Table 2.** Experimental values of the dispersion parameter, $E_d$, for the amorphous $Ge_xSb_{40-x}Se_{60}$ semiconducting alloy films, together with their corresponding experimental and theoretical values for the cation effective coordination number, $N_c$.

| Composition | $E_d$ (eV) | $N_c^{exp}$ | $N_c^{theo}$ |
|---|---|---|---|
| $Ge_{10}Sb_{30}S_{60}$ | 21.79 | 3.21 | 3.25 |
| $Ge_{20}Sb_{20}S_{60}$ | 22.78 | 3.42 | 3.50 |
| $Ge_{30}Sb_{10}S_{60}$ | 23.88 | 3.65 | 3.75 |

The values for the static refractive index, $n(0)$, have been calculated from the WDD dispersion parameters, $E_0$ and $E_d$, by using the formula (see equation (1))

$$n(0) = (1 + E_d/E_0)^{1/2}. \tag{4}$$

The compositional dependence of this particular optical parameter is shown in figure 3(*a*), for all the ternary alloy films under study. A slight increase has been obtained in the case of the films belonging to the $(As_{0.33}S_{0.67})_{100-x}Te_x$ compositional line, with increasing Te content, which can be straightforwardly explained by the larger atomic polarizability of Te atoms (with atomic radius of 137 pm), in comparison with the atomic polarizabilities of As and S atoms (with smaller atomic radii of 121 pm and 104 pm, respectively). Such a simple argument, based exclusively on the atomic polarizabilities of the different chemical elements, *does* also explain the slightly-downward linear trend in $n(0)$, for the films of the Ge–Sb–S glassy system, since the atomic polarizability of the Ge atoms (with atomic radius of 122 pm) is *smaller* than that corresponding to the Sb atoms (with a larger atomic radius of 140 pm).

### *3.2. Behaviour of the absorption coefficient*

Once the values of the refractive index are known in the whole working spectral region, in terms of equation (1),

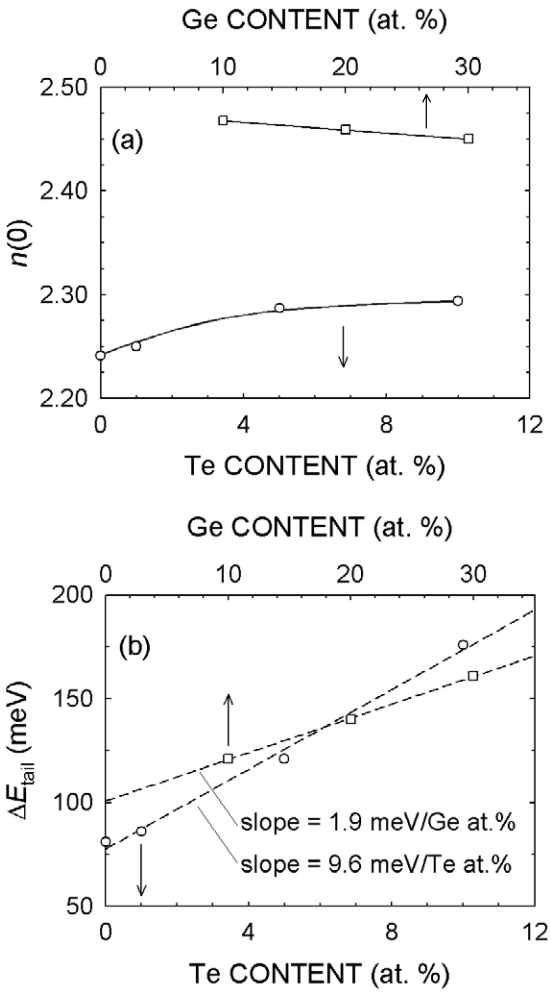


**Figure 3.** Compositional dependences of (*a*) $n(0)$ and (*b*) $\Delta E_{\rm tail}$, for the two ternary glassy systems under study.

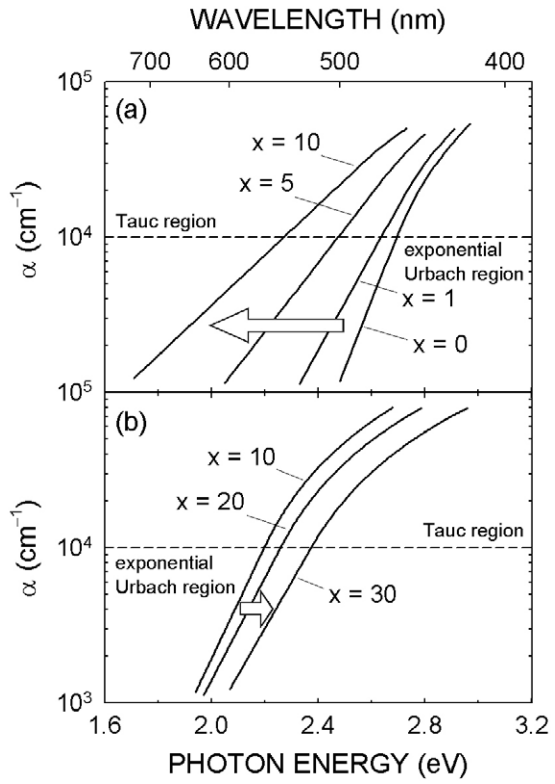


**Figure 4.** Optical-absorption spectra, $\alpha(\hbar\omega)$, of amorphous (*a*) $(As_{0.33}S_{0.67})_{100-x}Te_x$ and (*b*) $Ge_xSb_{40-x}S_{60}$ thin-film samples.

the optical-absorption spectra, $\alpha(\hbar\omega)$, of the ternary alloy films subjected to study were then derived from the *upper* envelope of their corresponding transmission spectra [10]. The calculated spectra of $\alpha$ are all displayed in figure 4, using a semi-logarithmic scale: in order to complete the computation of the optical constants $(n, k)$, the extinction coefficient, $k$, is easily determined from the already-known $\alpha$-values, using the formula, $k = \alpha\lambda/4\pi$. A clear red-shift of the optical-absorption edge is observed in figure 4, with increasing Te content, in the amorphous $(As_{0.33}S_{0.67})_{100-x}Te_x$ films (following the fundamental Kramers–Kronig relationships for $n$ and $k$, this red-shift in the absorption spectrum should give an increased refractive index, as experimentally observed), while a blue-shift occurs in the amorphous $Ge_xSb_{40-x}S_{60}$ samples, with increasing Ge content (in this case, the blue-shift in the absorption edge should give, instead, a decreased refractive index, as previously determined).

According to the 'non-direct electronic transition' model proposed by Tauc [17], the behaviour of the absorption coefficient in the strong-absorption region ($\alpha \gtrsim 10^4\,{\rm cm}^{-1}$), in amorphous semiconductors, is ruled by the equation

$$\alpha(\hbar\omega) = B\frac{(\hbar\omega - E_{\rm g}^{\rm opt})^2}{\hbar\omega}, \qquad (5)$$

where $B$ is a constant related to the parameter $\Delta E_{\rm tail}$, which is a measure of the extent of *band tailing*, and $E_{\rm g}^{\rm opt}$ is the already-introduced, optical band gap. Values of $B^{1/2}$ and $E_{\rm g}^{\rm opt}$ for the ternary alloy films have been derived by plotting $(\alpha\hbar\omega)^{1/2}$ versus $\hbar\omega$ (see figure 5), and they are all listed in table 1.

The *linear* compositional dependences of $E_{\rm g}^{\rm opt}$ for both glassy systems are also displayed as insets, in figure 5, along with their slopes, and it must be emphasized that remarkable differences have been found between both glassy systems. Thus, while $E_{\rm g}^{\rm opt}$ shows a notable decrease in the case of the amorphous As–S–Te films, with increasing Te content, it increases, instead, for the amorphous Ge–Sb–S samples, with increasing Ge content. Such different trends observed in $E_{\rm g}^{\rm opt}$ will be explained next, taking into account both the average molar bond energy values of the bonds present in the alloys and some structural aspects. Thus, it is well known that the structure of amorphous $As_{33}S_{67}$ films is mainly formed by basic $AsS_3$ pyramidal units, containing As–S heteropolar bonds (bond energy, 260 kJ mol$^{-1}$), linked through S–S homopolar bonds (bond energy, 280 kJ mol$^{-1}$). As already mentioned, it has been shown by Vlcek *et al* [15], Te joins the structure of amorphous $(As_{0.33}S_{0.67})_{100-x}Te_x$ alloy films, through the substitution of S atoms in the $AsS_3$ pyramidal units, to form additional $AsS_2Te$ mixed pyramidal units, containing lower bond energy As–Te bonds (bond energy, 205 kJ mol$^{-1}$). It is clearly inferred then, that the decrease found in $E_{\rm g}^{\rm opt}$ is related to the decrease in the As–S bond concentration and, in turn, to the subsequent increase in the As–Te bond concentration, with lower bond energy. Lastly, it should be pointed out that no evidence, whatsoever, of the presence of

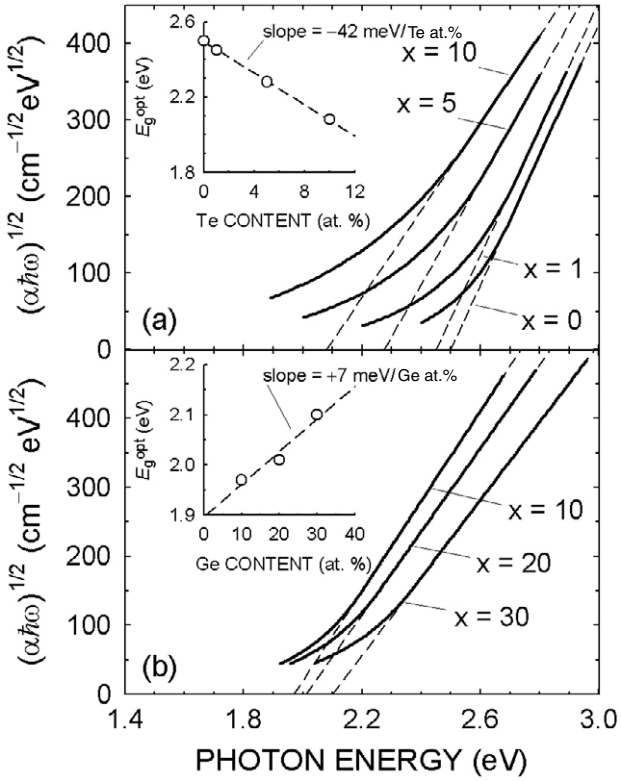


**Figure 5.** Determination of the optical band gaps in terms of Tauc's law, as linear extrapolation (dashed straight lines), of the high-absorption data. The linear compositional dependences of the Tauc gap, for the amorphous (*a*) $(As_{0.33}S_{0.67})_{100-x}Te_x$ and (*b*) $Ge_xSb_{40-x}S_{60}$ thin-film samples, are plotted in the corresponding insets.

S–Te bonds (bond energy, 195 kJ mol$^{-1}$) have been reported for the $(As_{0.33}S_{0.67})_{100-x}Te_x$ glassy system, in the case of *low* Te contents [15].

Amorphous Ge–Sb–S films, on the contrary, have a rather complex structure. It has been shown that a number of different structural units occur, depending on the Ge content. Thus, at low Ge contents, the structure is formed mainly by $SbS_3$ pyramidal units, containing Sb–S bonds (bond energy, 230 kJ mol$^{-1}$). In addition, $GeS_4$ tetrahedral units, containing higher bond energy Ge–S bonds (265 kJ mol$^{-1}$), appear when the Ge content is increased, which obviously contribute to increase the Tauc gap, as determined experimentally.

Should only the difference between the bond energies of Sb–S and Ge–S bonds be taken into account, an increase in the Tauc gap, $E_g^{opt}$, higher than that obtained experimentally, would be expected, with increasing Ge content. However, the addition of Ge to the $Sb_{40}S_{60}$ binary alloy produces new Sb–Sb and Ge–Ge homopolar bonds, with lower bond energies (175 kJ mol$^{-1}$ and 185 kJ mol$^{-1}$, respectively), which makes the upward trend in $E_g^{opt}$ smoother than initially expected.

The set of values of the Tauc slope, $B^{1/2}$, for all the ternary alloy films under study, is also listed in table 1. A significant decay is observed in this parameter, with increasing Te and Ge contents, respectively, in both glassy systems, which reflects an increase in the *degree of structural disorder*, in such amorphous alloys. Furthermore, the band-tailing parameter, $B$, is given, according to Mott and Davis [18], by the following expression:

$$B = \frac{4\pi\sigma_{min}}{n(0)c\Delta E_{tail}}, \qquad (6)$$

where $\sigma_{min}$ is the minimum electrical conductivity and $c$ is the light speed in vacuum. Assuming $\sigma_{min} = 350\,\Omega^{-1}\,cm^{-1}$, as a typical value for amorphous chalcogenide alloys, following Tichy *et al* [19,20], it is possible to *estimate* the localized-state tail widths, $\Delta E_{tail}$, of the amorphous semiconducting films under study. The linear compositional dependences of $\Delta E_{tail}$ for the amorphous $(As_{0.33}S_{0.67})_{100-x}Te_x$ and $Ge_xSb_{40-x}S_{60}$ films are both plotted in figure 3(*b*). The values of the band-tail width are expected to be, at least, around 0.1 eV in bulk glasses and in the more disordered thin films, even larger [19]. So, the values obtained in our study seem to be quite reasonable. It must also be pointed out that there is a large difference between the effects of the addition of Te and the addition of Ge, respectively, on the band-structure parameter $\Delta E_{tail}$ (one is nearly five times higher than the other, as can be seen in figure 3(*b*), where the two slopes corresponding to the two linear least-squares fits are indicated).

## 4. Concluding remarks

Amorphous $(As_{0.33}S_{0.67})_{100-x}Te_x$ (with $x = 0$, 1, 5 and 10 at.%) and $Ge_xSb_{40-x}S_{60}$ (with $x = 10$, 20 and 30 at.%) films have been successfully prepared by vacuum thermal deposition. The compositional dependences of the optical properties of all these ternary alloy films have been determined and discussed, in detail. It has been found that the addition of Te to the $As_{33}S_{67}$ binary alloy produces a very small decrease in the As (cation) effective coordination number, $N_c$, which is clearly consistent with previously reported structural studies, showing that the 'layered structure' of these alloys remains almost unaltered, at low Te contents: Te joins the structure through the substitution of S atoms in the $AsS_3$ pyramidal units, to form new $AsS_2Te$ mixed pyramidal units. On the contrary, amorphous $Ge_xSb_{40-x}S_{60}$ films show a remarkable increase in the structural parameter $N_c$, which has been explained by the presence of, on the one hand, $GeS_4$ tetrahedral units, and, on the other hand, $S_3Ge$–$GeS_3$ 'quasi-tetrahedral' units, when the Ge content is increased. Furthermore, it has to be stressed that the formation of Ge–Ge and Sb–Sb homopolar bonds makes the increase in $N_c$ smoother than that theoretically expected. Structural modifications stemming from changes in the chemical composition of the material also lead to important changes in the case of the Tauc gap. Thus, it has been derived that $E_g^{opt}$ decreases substantially, with increasing Te content, in As–S–Te films, while it increases, instead, in the case of Ge-based ternary alloys, with increasing Ge content. Last but not the least, the present study clearly reveals that the addition of the elements Te and Ge, respectively, significantly increases the degree of structural disorder in both glassy semiconducting systems, although it is obviously much more appreciable in the case of the addition of Te to the $As_{33}S_{67}$ chalcogenide alloy.

## Acknowledgments

This work has been partly supported by the MCYT (Spain) and FEDER (EU), under MAT2001-3333 research project, and a Marie Curie European Reintegration Grant, of the Sixth Framework Programme, under contract MERG-CT-2004-507791.

## References

[1] Savage J A 1985 *Infrared Optical Materials and their Antireflection Coatings* (Bristol: Hilger)
[2] Elliott S R 1990 *Physics of Amorphous Materials* 2nd edn (New York: Longman)
[3] Popescu M A 2000 *Non-Crystalline Chalcogenides* (Dordrecht: Kluwer)
[4] Wagner T, Márquez E, Fernández-Peña J, González-Leal J M, Ewen P J S and Kasap S O 1999 *Phil. Mag.* B **79** 223
[5] Prieto-Alcón R, Márquez E, González-Leal J M, Jiménez-Garay R, Kolobov A V and Frumar M 1999 *Appl. Phys.* A **68** 653
[6] Márquez E, Ramírez-Malo J B, Fernández-Peña J, Jiménez-Garay R, Ewen P J S and Owen A E 1993 *Opt. Mater.* **2** 143
[7] Márquez E, Wagner T, Bernal-Oliva A M, González-Leal J M, Prieto-Alcón R and Vlcek M 2000 *J. Non-Cryst. Solids* **274** 62
[8] Ohta T and Ovshinsky S R 2003 *Photo-Induced Metastability in Amorphous Semiconductors* ed A V Kolobov (Weinheim: Wiley-VCH) p 310
[9] González-Leal J M, Krecmer P, Prokop J and Elliott S R 2003 *Photo-Induced Metastability in Amorphous Semiconductors* ed A V Kolobov (Weinheim: Wiley-VCH) p 338
[10] González-Leal J M, Prieto-Alcón R, Ángel J A, Minkov D A and Márquez E 2002 *Appl. Opt.* **41** 7300
[11] Swanepoel R 1984 *J. Phys. E: Sci. Instrum.* **17** 896
[12] McClain M, Feldman A, Kahaner D and Ying X 1991 *Comput. Phys*. **5** 45
[13] Wemple S H and DiDomenico M 1971 *Phys. Rev.* B **3** 1338
[14] Wemple S H 1973 *Phys. Rev.* B **7** 3767
[15] Mir. Vlcek, Nejezchleb K, Wagner T, Frumar M, Mil. Vlcek, Vidourek A and Ewen P J S 1998 *Thin Solid Films* **317** 228
[16] Kotsalas I P, Papadimitriou D, Raptis C, Vlcek M and Frumar M 1998 *J. Non-Cryst. Solids* **226** 85
[17] Tauc J 1974 *Amorphous and Liquid Semiconductors* ed J Tauc (New York: Plenum) p 159
[18] Mott N F and Davis E A 1979 *Electronic Processes in Non-Crystalline Materials* 2nd edn (Oxford: Clarendon)
[19] Tichy L, Ticha H, Nagels P and Callaerts R 1998 *Mater. Lett.* **36** 294
[20] Tichy L, Ticha H, Nagels P and Callaerts R 1998 *J. Non-Cryst. Solids* **240** 177